Aerospace Science and Technology 14 (2010) 575–586

Contents lists available at ScienceDirect

Aerospace Science and Technology

www.elsevier.com/locate/aescte

An experimental investigation on the aerodynamic performances of flexible membrane wings in flapping flight

Hui Hu [a,*], Anand Gopa Kumar [a], Gregg Abate [b], Roberto Albertani [c]

[a] Department of Aerospace Engineering, Iowa State University, Ames, IA 50011, United States
[b] Air Force Research Laboratory, Elgin Air Force Base, FL, United States
[c] University of Florida Research & Engineering Education Facility, Shalimar, FL, United States

ARTICLE INFO

Article history:
Received 2 September 2009
Received in revised form 29 April 2010
Accepted 5 May 2010
Available online 8 May 2010

Keywords:
Unsteady aerodynamics
Flapping wing
Membrane wing
Flexible wings

ABSTRACT

An experimental study was conducted to assess the aerodynamic benefits of flapping flight compared with fixed-wing soaring flight for the development of flapping-wing Micro-Air-Vehicles (MAVs). The time-averaged aerodynamic performances (i.e. mean lift and thrust/drag) of two flexible membrane wings with different skin flexibility (i.e., a flexible nylon wing and a very flexible latex wing) were compared with that of a conventional rigid wing to evaluate the effects of skin flexibility of the tested wings on their aerodynamic performances for flapping flight applications. The measurement results revealed clearly that, for all the tested wings, flapping motion would bring significant aerodynamic benefits when the flapping flight is in unsteady state regime with advance ratio (i.e., the ratio of forward flight speed to wingtip velocity) of the flapping flight being smaller than 1.0. The aerodynamic benefits of flapping flight were found to decay rapidly as the advance ratio increases. The skin flexibility of the tested wings was found to have considerable effects on their aerodynamic performances for both soaring and flapping flights: The flexible membrane wings were found to have better overall aerodynamic performance (i.e., lift-to-drag ratio) over the rigid wing for soaring flight, especially for high speed soaring flight or at relatively high angle of attack. The rigid wing was found to have better lift production performance for flapping flight in general. The latex wing, which is the most flexible among the three tested wings, was found to have the best thrust generation performance for flapping flight. The less flexible nylon wing, which has the best overall aerodynamic performance for soaring flight, was found to be the worst for flapping flight applications.

1. Introduction

Micro-Air-Vehicles (MAVs), which are characterized by small vehicle size (<15 cm) and low flight speed (<10 m/s), have attracted a growing interest in aerospace engineering community due to their great potentials for various civil and military applications. Equipped with video cameras, transmitters, or sensors, these miniaturized aerial vehicles can perform surveillance, reconnaissance, targeting, or biochemical sensing tasks at remote, hazardous, or dangerous locations. Although scaled-down versions of conventional designs of "macro-scale" aircraft may be the obvious approach to MAV design and are being pursued for many outdoor applications, such flight platforms are unattractive for indoor flight for a number of reasons. Fixed-wing MAVs, for example, do not have the required agility for obstacle-avoidance in indoor flight, and are incapable of hovering. Although rotary-wing MAVs offer good agility and vertical-take-off-and-landing (VTOL) capability, they suffer from wall-proximity effects, are too noisy, and usually inefficient for low Reynolds number flight [6,26]. A plausible alternative, therefore, is flapping flight.

Flapping flight is one of the most complex yet widespread modes of transportation found in nature. Over a million different species of insects fly with flapping wings to produce lift and thrust, and more than 10,000 different kinds of birds and bats flap their wings for locomotion [7]. Flapping flight has undoubtedly been a sophisticated realm of flight and has intrigued human beings for hundreds of years. It has long been realized that steady-state aerodynamics does not accurately account for the aerodynamic forces produced by the flapping flight of natural fliers. This has prompted extensive studies to uncover the underlying physics and to elucidate fundamental mechanisms employed by the natural fliers to produce enough aerodynamic forces needed for propulsion and maneuvering. Much progress has already been made in recent years associated with the flapping flight of the natural fliers. As summarized by Viieru et al. [38], the fundamental mechanisms responsible for high lift generations in flapping flight would include: 1) Weis-Fogh's clap-and-fling [40,20,21]; 2) delayed dynamic stall associated with leading-edge vortex attachment in flapping mo-

* Corresponding author.
E-mail address: huhui@iastate.edu (H. Hu).

1270-9638/$ – see front matter
doi:10.1016/j.ast.2010.05.003

tion [10,8]; 3) fast pitching-up rotation of flapping wings [9,34,35]; and 4) wake capturing associated with wing–wake interaction during flapping flight [9,34,35,39]. Further information about unsteady aerodynamics of flapping flight can be found from the reviews of Ho et al. [14], Ansari et al. [4], Mueller [22], and Shyy et al. [30].

Although much progress has already been made about flapping flight, most of the previous studies were conducted from a biologist's point of view to try to understand the fundamental mechanism of the flapping flights of natural fliers. As described by Mueller and DeLaurier [22], there is a fundamental difference between an aerospace engineer's interest in flapping flight and that of a biologist or zoologist. The primary motivation for studying the flight mechanics of natural fliers is to explain the physics for a creature that is known to fly. The fact that it achieves successful thrust and propulsion is given. Therefore, various analytical models are adjusted to match the measurement results, and conclusions are reached regarding energetic, migration capabilities, etc. An aerospace engineer, in contract, is trying to develop a flying aircraft, and its ability to achieve this is not a given fact. What an aerospace engineer needs is a design-oriented analysis, which is not what can be offered from animal-flight studies.

Numerous experimental and numerical studies have been conducted in recent years to investigate the flow pattern and vortex structures in the wakes of flapping airfoil/wings. Much work has also been done to study the variations of the resultant aerodynamic forces (lift and thrust) acting on flapping airfoils/wings with phase angle of up-stroke and down-stroke within a flapping cycle. However, very little in the literature can be found to quantify the overall aerodynamic performances of flapping wings (i.e., how much time-averaged lift and thrust can be generated by flapping the airfoils/wings) as functions of flapping frequency, forward flight speed, as well as the orientation angle of the flapping plane with respect to incoming flows (i.e., flight direction). For the development of engineered flapping-wing-based MAVs, such information is extremely important because the performances of MAVs, such as the vehicle size, payload, and flight speed, would be totally determined by the mean lift and thrust that can be produced by the flapping wings.

Thin and flexible membrane wings are unique to flying mammals such as bats, flying squirrels, and sugar gliders. These animals exhibit extraordinary flight capabilities with respect to maneuvering and agility that are not observed in other species of comparable size. It has been suggested that a potentially useful feature for engineered maneuverable MAVs might be the incorporation of flexible membranes as lifting surfaces. With this in mind, we conducted the present study to try to leverage the unique feature of flexible membrane airfoils/wings found in bats and other flying mammals to explore the potential applications of such non-traditional bio-inspired flexible-membrane airfoils/wings to MAV designs for improved aerodynamic performance. It should be noted that several successful efforts have already been made in recent years to adopt flexible membrane airfoils/wings in the designs of functional MAVs [2,1,28]. It has been found that flexible membrane airfoils/wings are able to alleviate the effects of gust wind, delay airfoil stall, and provide additional advantages for morphing to achieve enhanced agility and storage compared to conventional rigid airfoils/wings for MAV applications [2,1,28,27,29,31,16,32]. However, most of the previous studies on flexible membrane wings/airfoils are targeted for fixed-wing MAV designs, only a few studies were conducted recently to investigate the effects of the skin flexibility of membrane airfoils/wings on their aerodynamic performances for flapping-wing MAV applications [12,13,17]. Based on the particle image velocimetry and force measurements of three airfoils with different bending stiffness, Heathcote et al. [12] found that the strength of the wake vortices, their lateral spacing, and the time-averaged velocity of the induced jet would depend on the airfoil flexibility, plunge frequency, and amplitude. They also found that there exist an optimum airfoil stiffness for a given plunge frequency and amplitude, and the thrust/input-power ratio would be greater for flexible airfoils than for rigid airfoil. While it has been suggested that flexibility may benefit flapping-wing MAVs both aerodynamically and in the inherent lightness of flexible structures [13], much work is still needed to fully explore the advantages or disadvantages of using flexible membrane airfoils/wings for flapping-wing MAV designs.

In the present study, an experimental investigation was conducted to assess the aerodynamic benefits of using flexible membrane airfoils/wings for flapping-wing MAV applications. The time-averaged lift and thrust generated by flapping two flexible membrane wings with different skin flexibility were compared with those of a conventional rigid wing to quantify the effects of the skin flexibility of the tested wings on their aerodynamic performances. During the experiments, the time-averaged lift and thrust generated by the tested wings as the functions of flapping frequency, forward flight velocity, and the orientation angle of the flapping plane with respect to the incoming flows were measured by using a high sensitivity force-moment sensor. Advance ratio, which is defined as the ratio of the forward flight speed to the wingtip velocity of the tested wings in flapping flight, was used to characterize measurement data to assess the aerodynamic advantages of flapping flight over soaring flight (i.e., without flapping motion) for MAV applications.

2. Experimental setup and studied wings

The experiments were performed in a low-speed wind tunnel located in the University of Florida's Research & Engineering Education Facility (UF-REEF) near Air Force Research Laboratory at Eglin Air Force Base. The wind tunnel has a bell mouth inlet with the inlet cross sectional being 3.7 m × 3.7 m. A flow conditioning section consisted of honeycomb screens and mesh structures were installed ahead of a contraction section to provide uniform, low-turbulent incoming flow to enter the test section. The exit of the contraction section is a 1.1 m × 1.1 m in square, which is the start of the open jet test section. The open jet test section has a rigid enclosure of 3.4 m high × 3.7 m wide × 4.6 m long. A diffuser section is installed at the downstream of the open jet test section to make a transition from a square cross-section to a 1.5 m (diameter) circular axial fan driven by a 50 HP Reliance Electric motor.

Fig. 1 shows the test rig and flapping mechanism used in the present study. Similar to the work of Hong and Altman [15], the flapping mechanism used in the present study was adapted from a Cybird-P1® remote control ornithopter model, which is powered by a DC power supply. During the experiments, the flapping frequency of the mechanism is adjustable by changing the output voltage of the DC power supply. The aerodynamic forces (lift, and thrust or drag) acting on the tested wings were measured by using a high-sensitive force-moment sensor cell (JR3, model 30E12A-I40). The force-moment sensor cell is composed of foil strain gage bridges, which are capable of measuring the forces on three orthogonal axes and the moment (torque) about each axis. The precision of the force-moment sensor cell for force measurements is about ±0.05% of the full scale (40 N). During the experiments, the output signals from the force-moment sensor cell were scanned at 1000 Hz for 60 seconds for each tested case. It should be noted that, while much more other information such as the variations of the aerodynamic forces (i.e., lift and thrust or drag) acting on the flapping wings with the phase angle of up-stroke and down-stroke in flapping cycles can be derived quantitatively from the acquired 60,000 data samples for each tested case, only the time-averaged lift and thrust (or drag) data were shown in the present study to

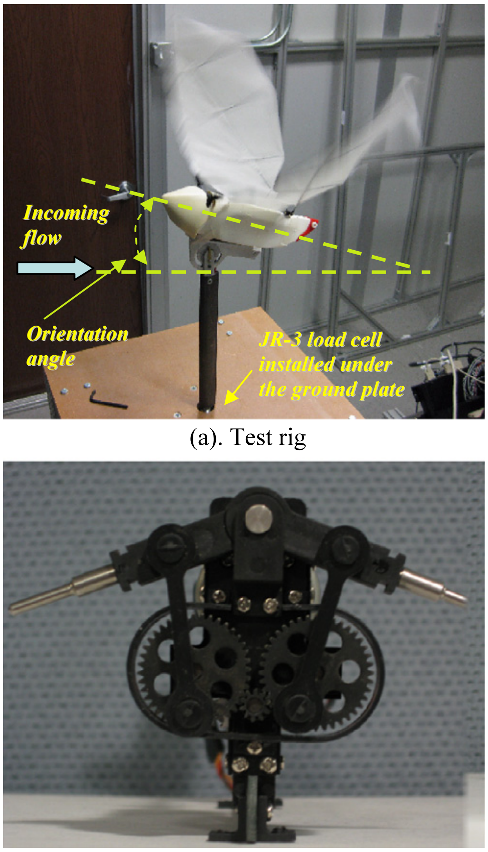

(a). Test rig

(b). Flapping mechanism

Fig. 1. Test rig and flapping mechanism used in the present study.

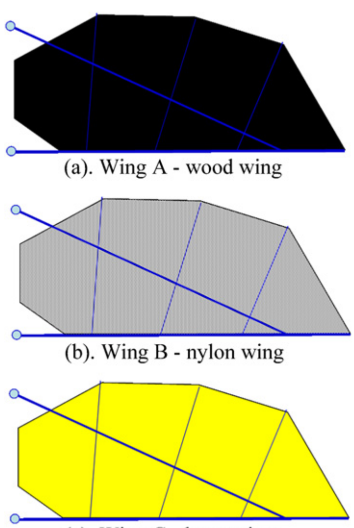

(a). Wing A - wood wing

(b). Wing B - nylon wing

(c). Wing C - latex wing

Fig. 2. The tested wings.

assess the effects of the skin flexibility on the overall aerodynamic performances of the flapping wings.

Fig. 2 shows the schematic of the three wing models used in the present study. All the three tested wings have the same rigid glass fiber frames (i.e., rigid leading edge spar and chordwise battens, mass 12.0 gram) and same elliptical wing planform shape and dimensions. The skin flexibility of the wings is quite different. The wing model-A is a rigid wing, which is made of a thin wood plate (thickness ∼200 μm). The rigid wood wing was used as the comparison baseline in the present study in order to assess the aerodynamic benefits of using flexible membrane wings for soaring flight and flapping flight. The wing model-B is a flexible membrane wing, which is made of a thin nylon film (thickness ∼70 μm) bonded to the rigid graphite frame. The skin of nylon wing, which has much less bending stiffness than axial stiffness, could deform along both chordwise and spanwise directions during soaring and flapping flight. The wing model-C is made of a thin latex sheet (thickness ∼120 μm) bonded to the same rigid graphite wing frame, which has comparable bending and axial stiffness. Following the work of Heathcote et al. [12], bending stiffness, $K = Eb^3/12$, is used in the present study to quantify the flexibility of the flapping wing, where E is the modulus of elasticity of the material and b is the thickens of the wing. The bending stiffness ratio of the three tested wings is $k_1 : k_2 : k_3 = 2800 : 15 : 1$. Therefore, the three tested wings used in the present study are referred to as "rigid", "flexible", and "very flexible", respectively. Further information about the characteristics of the tested wings is listed in Table 1.

Table 1
The design parameters of the tested wings.

Tested wing	Mass (g)	Area of wing platform (cm^2)	Wing span (cm)	Chord at mid-span (cm)	Flapping angle (deg.)
Rigid wing	59.7	475.1	36.8	16.5	47.4
Nylon wing	15.1	475.1	36.8	16.5	47.4
Latex wing	30.0	475.1	36.8	16.5	47.4

3. Experimental results and discussions

3.1. Aerodynamic performances of the tested wings in soaring flight

The aerodynamic performances of the three tested wings were compared at first for soaring flight (i.e., fixed wing) applications. During the experiments, the rigid leading edges of the tested wings were positioned horizontally. The incoming flow velocity in the test section (i.e., the forward flight speed) was varied from 1.0 m/s to 10.0 m/s, and the corresponding chord Reynolds number (based on the chord at wing mid-span) $Re_C \approx 10{,}000$ to 100,000. For soaring flight, the orientation angle (OA) shown in Fig. 1 is actually the angle of attack of the tested wings with respect to the incoming flows. Fig. 3 and Fig. 4 show some typical measurement results of the tested wings with the soaring flight speed $V_\infty = 2.0$ m/s ($Re_C \approx 20{,}000$) and $V_\infty = 8.0$ ($Re_C \approx 80{,}000$) m/s, respectively. The error bars shown in the plots represent the standard deviations of the measurement data over time.

As revealed from the experimental data given in Fig. 3, when the flight speed is relatively low (i.e., $V_\infty = 2.0$ m/s), all the three tested wings were found to have very comparable aerodynamic performances (in terms of lift and drag coefficients) at relatively small orientation angles (i.e., OA $<$ 10.0 deg.). The flexible membrane wings were found to have slightly larger lift and drag coefficients compared with the rigid wood wing at relatively high orientation angles (i.e., OA $>$ 10.0 deg.).

This can be explained by that, when the forward flight speed is relatively low, the aerodynamic forces acting on the tested wings would be relatively small, especially at relatively low orientation angles (i.e., OA $<$ 10.0 deg.). No apparent deformations were found on the flexible membrane wings (for both the nylon wing and the latex wing). As a result, the flexible membrane wings were found to have very comparable aerodynamic performances to those of the rigid wood wing at low soaring flight speed with relatively low orientation angle (i.e., OA $<$ 10.0 deg.).

When the orientation angle becomes more significant (i.e., OA $>$ 10.0 deg.), obvious deformations were observed for the tested flexible membrane wings due to the increased aerodynamics forces acting on the tested wings. The straight chords of the

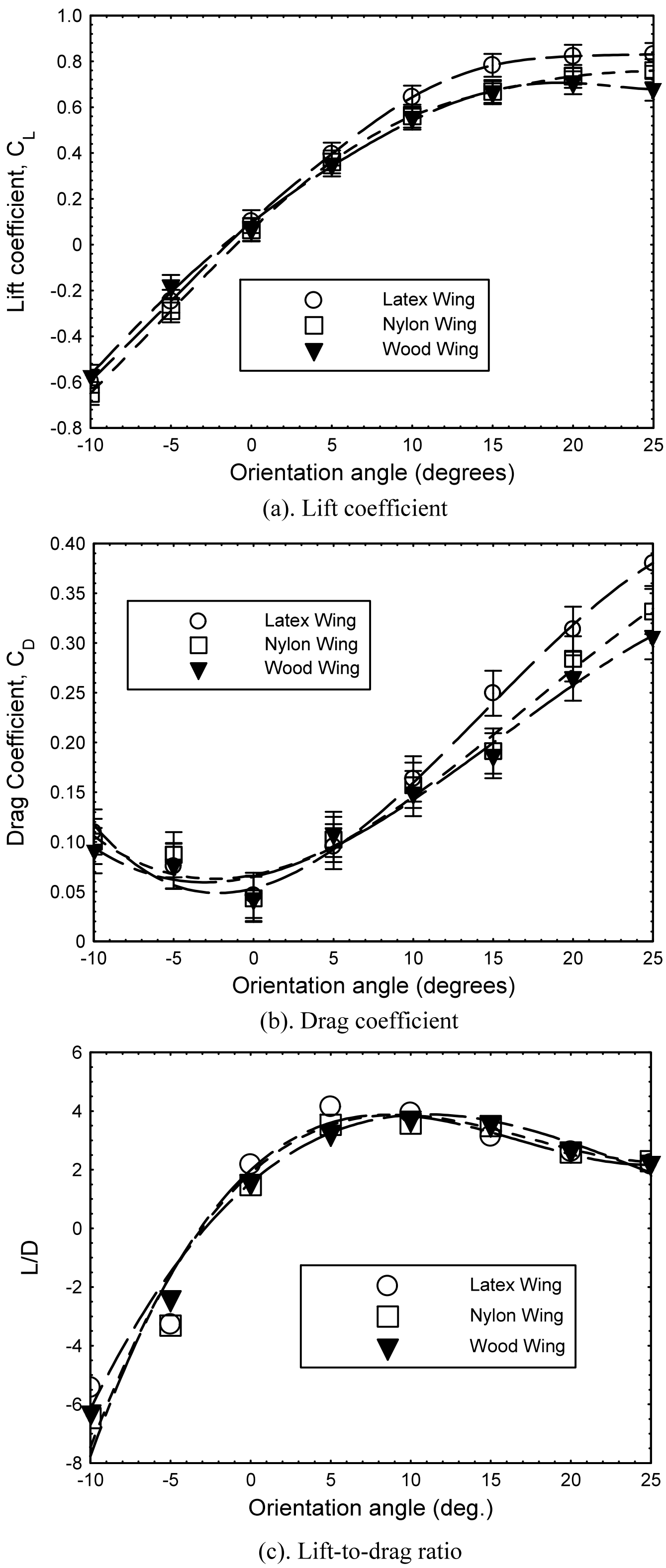

Fig. 3. The tested wings in soaring flight with forward flight speed $V_\infty = 2.0$ m/s ($Re_C \approx 20{,}000$).

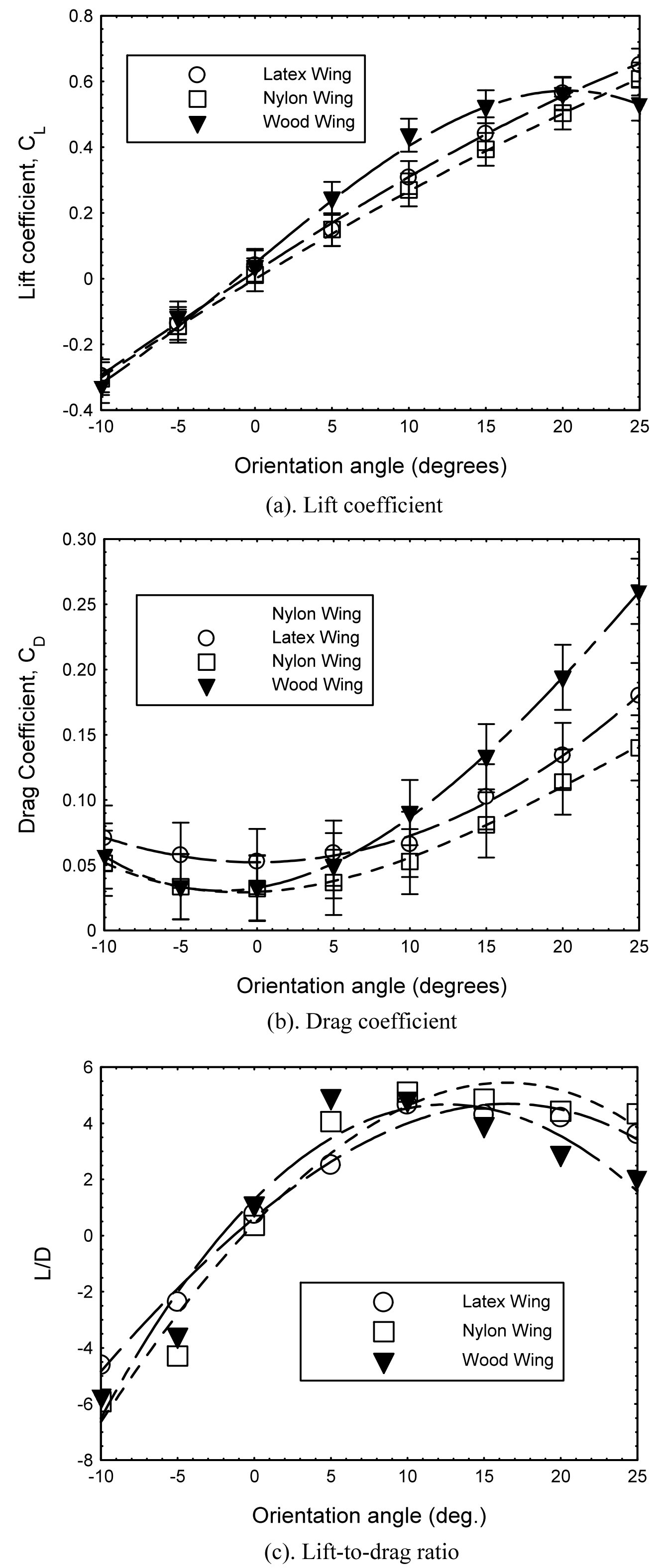

Fig. 4. The tested wings in soaring flight with forward flight speed $V_\infty = 8.0$ m/s ($Re_C \approx 80{,}000$).

flexible membrane wings were found to be curved slightly (i.e., to have small chordwise cambers) when the orientation angle becomes relatively high (i.e., OA < 10.0 deg.). As a result, the flexible membrane wings were found to have slightly larger lift and drag coefficients compared with those of the rigid wood wing. Due to its more flexible skin, the latex wing was found to deform more seriously (i.e., the straight chord was curved more obviously to have larger cambers) compared with the nylon wing. Therefore, the lift coefficients of the latex wing were found to be slightly larger than the nylon wing at relatively higher orientation angles. It was also found that the trailing edge of the flexible latex wing was fluttering when the orientation angle becomes relatively high during the soaring flight experiments. The fluttering of the trailing edge of the flexible latex wing was found to become more and more significant with increasing orientation angle. This is believed to be the reason why the drag coefficients of the latex wing were found to increase more rapidly with the increasing orientation angle compared with the rigid wood wing and the less flexible nylon wing.

Although the straight chords of the flexible wings were found to be curved slightly to have small chordwise cambers, the induced deformations on the flexible membranes wings (for both latex and nylon wings) were still quite limited when the soaring flight speed is relatively low since the aerodynamic forces acting on the tested wings were still relatively weak. As revealed from the lift-to-drag ratio data given in Fig. 3(c), the lift-to-drag ratios of all three tested wings were found to be very comparable for the soaring flight with relatively low soaring flight speed.

As the soaring flight speed increases, the aerodynamic forces acting on the tested wings would become larger and larger. As reported by Hu et al. [16], the significant aerodynamic forces acting on flexible membrane airfoils/wings would cause chordwise profile changes to adapt the incoming flows (i.e., the chord profiles of the flexible membrane wings would be adjusted automatically) to balance the pressure differences between the upper and lower surfaces of the flexible membrane airfoils/wings. When the aerodynamic forces acting on flexible membrane airfoils/wings become more significant, the trailing edges of the flexible membrane airfoils/wings would be deflected and lifted up from its original designed position, which would reduce the effective angle of attack of the flexible membrane airfoils/wings with respect to incoming flows. Similar phenomena were also observed in the present study when the soaring flight speed becomes relatively high ($V_\infty > 6.0$ m/s).

Fig. 4 shows the measured lift coefficients, drag coefficients, and lift-to-drag ratio of the three tested wings at relatively high soaring flight speed (i.e., $V_\infty = 8.0$ m/s). During the experiments, the deformations on the tested flexible membrane wings (for both latex and nylon wing) were found to become very serious. Due to the more significant aerodynamic forces acting on the tested wings, in additional to having the straight chords of the flexible membrane wings curved more seriously, the trailing edges of the flexible membrane wings were also found to be deflected and lifted from their design position substantially, especially at relatively high orientation angles (i.e., OA > 10.0 deg.). Since the effective angles of attack of the tested flexible membrane wings with respect to the incoming flows were reduced considerably due to the trailing edge deflection, the lift coefficients of the flexible membrane wings were found to be slightly smaller than those of the rigid wood wing.

As revealed from the measurement results given in Fig. 4(a), the lift coefficient profile of the rigid wood wing was found to reach its peak value at OA ≈ 20.0 deg., then begin to decrease. It indicates that stall would occur at OA ≈ 20.0 degrees for the rigid wood wing. On the other hand, the lift coefficients of the flexible membrane wings (both the latex and nylon wings) were found to increase monotonically with the increasing orientation angle up to OA = 25.0 deg. Such measurement results indicate that the flexible membrane airfoils could delay stall to a higher orientation angle, which agrees with the finding of Stanford et al. [33], who conducted wind tunnel experiments to investigate the aerodynamic performance of flexible membrane airfoils/wings for fixed-wing MAV applications.

As visualized by the PIV measurements of Hu et al. [16], the flexible membrane wings would change their chordwise profiles automatically to adapt to incoming flows to suppress large flow separation. The deflection of their trailing edges would also reduce the effective angle of attack of the wings with respect to the incoming flows substantially. As a results, the drag coefficients of the flexible membrane wings were found to be much smaller compared with those of the rigid wing at relatively high orientation angles (i.e. OA > 10.0 deg.). Since the trailing edges of the latex wing were found to be fluttering at almost all the tested orientation angles, therefore, the drag coefficients of the latex wing were found to be slightly bigger than those of the nylon wing. From the lift-to-drag ratio profiles given in Fig. 4(c), it can be seen clearly that flexible membrane wings would have better overall aerodynamic performances compared with the rigid wood wing in general, especially at relatively high orientation angles (OA > 10.0 deg.).

In summary, the measurement results confirmed that flexible membrane wings could provide better aerodynamic performance compared with conventional rigid wing for soaring flight or fixed-wing MAV applications, as reported in previous studies [16,33]. The aerodynamic benefits of using flexible membrane wings for soaring flight are more highlighted for the cases with relatively high soaring speed and high angles of attack, where the induced deformation on the flexible membrane wings become more significant. The nylon wing, which is less flexible than the latex wing, was found to have the best overall aerodynamic performance among the three tested wings for soaring flight. This implies that it is important to choose a proper flexibility of the membrane skins in order to achieve improved aerodynamic performance by using flexible-membrane airfoils/wings for fixed-wing MAV applications.

3.2. Aerodynamic performances of the tested wings in flapping flight

It is well known that a wing in flapping motion will also experience inertial force in addition to aerodynamic forces. As described in Isaac et al. [18], the instantaneous inertial force acting on a flapping wing is a function of many parameters, which include the mass of the test wing, the flapping frequency, and angular displacement (i.e., phase angle). Since the purpose of the present study is to assess the effects of the skin flexibility on the time-averaged aerodynamic performances (i.e., mean lift and drag) of the flapping wings, only the time-averaged mean inertial force is of interest to the present study. While the instantaneous inertial force acting on the flapping wing may vary significantly during each cycle of the flapping motion, most of the inertial force in the up strokes will be canceled out by that in the down strokes [15]. Based on the work of Isaac et al. [18], the mean inertial force induced by flapping motion, $\overline{F}_{inertial}$, can be expressed as:

$$\overline{F}_{inertial} \propto CMf^2 \tag{1}$$

where C is a parameter representing the characteristics of the flapping motion; M is the mass of the flapping wing, and f is the flapping frequency. The value of C will become zero (i.e., $C = 0$) for a symmetric flapping motion since the inertial force in the up strokes will be canceled out by those in the down strokes completely.

An experiment was conducted in present study to determine the value of the parameter, C, for the flapping mechanism used in the present study. By flapping the rigid glass fiber frames (12.0 gram in mass) which were used to make the test wings, the mean inertial force induced by the flapping motion of the rigid glass fiber frames only (i.e., without any skins, thereby, almost no aerodynamic force) were measured as a function of the flapping frequency, which is shown in Fig. 5. The measured mean inertial force data were found fit to a square function reasonably well, as it is expected theoretically. By using the value of the parameter, C, derived from the curve fitting given in Fig. 5, the mean inertial forces acting on the test wings (i.e., glass fiber frames plus skins) at different flapping frequencies were estimated based on Eq. (1) and the mass data of the tested wings as listed in Table 1. It was found that the magnitudes of the estimated mean inertial forces of the

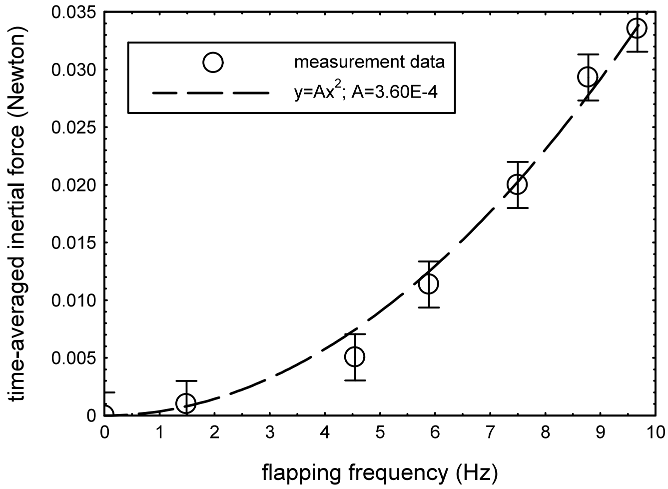

Fig. 5. Time-averaged inertial force of the rigid glass fiber frame vs. flapping frequency.

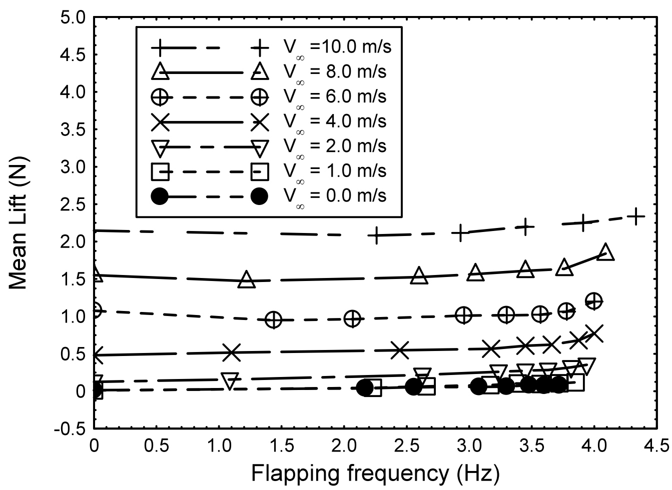

(a). Mean lift

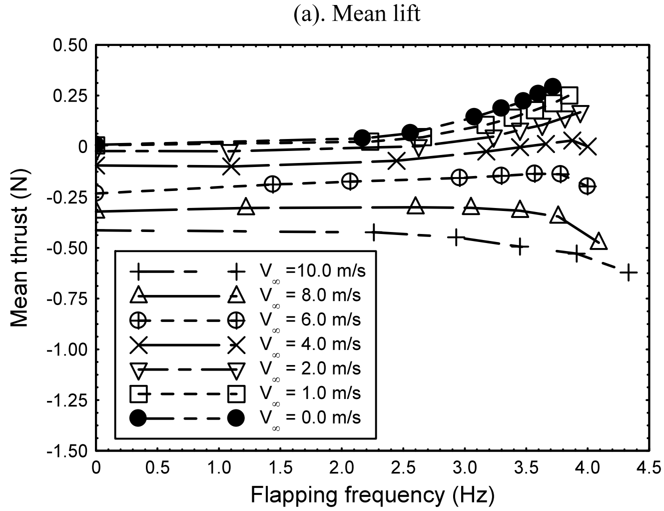

(b). Mean thrust

Fig. 6. Lift and thrust produced by the rigid wood wings in flapping flight at OA = 10.0 deg.

tested wings were usually quite small for the present study, which was less than 5.0% of those of the measured aerodynamic forces. In the present study, the estimated mean inertial forces acting on the test wings at different flapping frequencies were subtracted from the force measurement results to correct the effects of the mean inertial forces on measured aerodynamic force data.

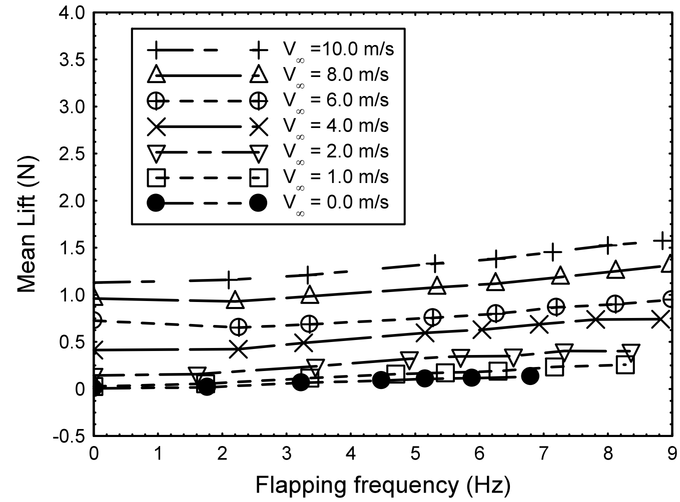

(a). Mean lift

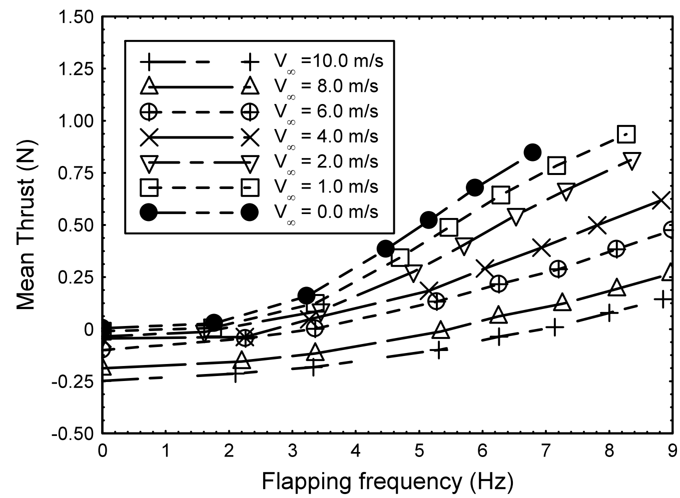

(b). Mean thrust

Fig. 7. Lift and thrust produced by the flexible nylon wing in flapping flight at OA = 10.0 deg.

For flapping flight experiments, the forward flight speed (i.e., the incoming flow velocity) was changed from 1.0 to 10.0 m/s. The orientation angle of the flapping motion with respect to the incoming flow was changed from −10.0 degrees to 20.0 degrees. Figs. 6 to 8 show the time-averaged lift and thrust produced by the three tested wings as functions of the flapping frequency with the orientation angle OA = 10.0 degrees. It should be noted the negative thrust data shown in the plots represent that the aerodynamic forces acting on the tested wings are actually drags instead of thrust. It should also be noted that the measurement results with zero flapping frequency (i.e., $f = 0.0$ Hz) represent those when the tested wings was in soaring flight. As expected, the drag (i.e., negative thrust) acting on the tested wings were found to increase with the increasing forward flight speed for soaring flight (i.e., $f = 0.0$ Hz) cases.

The measurement results revealed that, with the same forward flight speed, the time-averaged lift produced by flapping motion will increase with the increasing flapping frequency monotonically. For the same tested wings and the same flapping frequency, the time-averaged lift produced by flapping motion was found to increase as the forward flight speed increases.

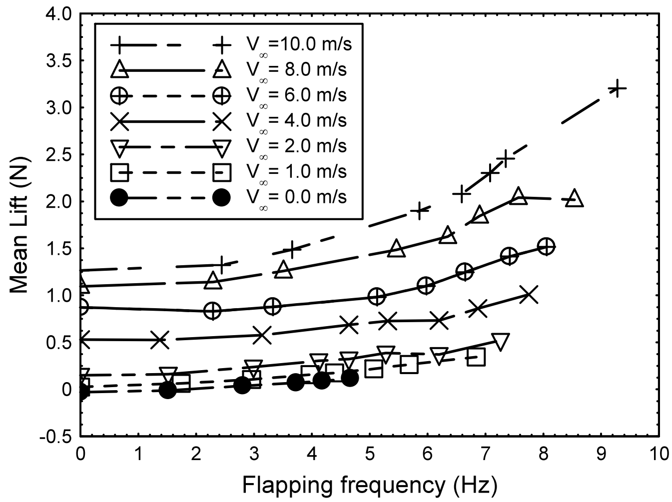

(a). Mean lift

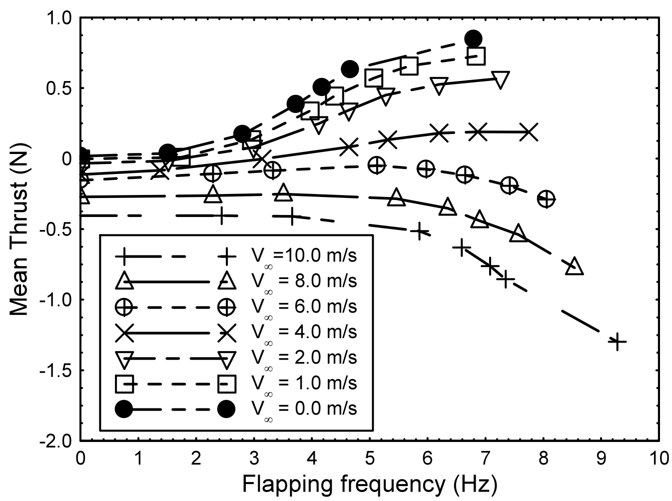

(b). Mean thrust

Fig. 8. Lift and thrust produced by the flexible latex wing in flapping flight at OA = 10.0 deg.

As revealed from the measurement data given in Fig. 7(b), the time-averaged thrust generated by flapping the nylon wing was found to increase monotonically with the increasing flapping frequency for all the tested cases with the forward flight speed changing from 0 (i.e., hovering flight) to 10.0 m/s. With the same flapping frequency, the time-averaged thrust generated by the flapping motion was found to decrease rapidly with the increasing forward flight speed.

Surprisingly, the time-averaged thrust generated by flapping the rigid wood wing (Fig. 6(b)) and the very flexible latex wing (Fig. 8(b)) were found to increase with the increasing flapping frequency only when the forward flight speed is relatively low ($V_\infty < 6.0$ m/s). When the forward flight speed becomes relatively high ($V_\infty \geqslant 6.0$ m/s), the thrust generated by flapping the wings was found to be decreasing as the flapping frequency increases. As mentioned above, the negative thrust data indicate that the aerodynamic forces acting on the tested wings are actually drag forces. The measurement results shown in Fig. 6(b) and Fig. 8(b) revealed that, when the forward flight speed became relatively high ($V_\infty \geqslant 6.0$ m/s), it would produce much larger drag forces (instead of thrust) when the rigid wing and the latex wing were flapping with higher flapping frequency. Such measurement results revealed that additional drag will be induced by flapping the wings compared with those without flapping motion (i.e., soaring flight with $f = 0$ Hz) when the forward flight speed becomes relatively high ($V_\infty \geqslant 6.0$ m/s). Although the nylon wing was still found to generate thrust in flapping flight, the thrust generation due to the flapping motion (i.e., the difference between the time-averaged thrust/drag forces in flapping flight and those of the soaring flight) was found to decrease rapidly as the forward flight speed increases. All these measurement results indicate that the advantages of flapping flight for both lift augmentation and thrust generation would be diminished as the forward flight speed increases. Such findings may also be used to explain why low-speed fliers such as humming birds and insects (their flying speed are usually relatively low) flap their wings all the time, while high-speed fliers such as eagles and seagulls hardly flap their wings during their high speed flights.

In order to quantify the aerodynamic benefits of flapping flight over soaring flight more clearly, we introduce the concepts of lift augmentation ($\Delta L_{flapping}$) and thrust augmentation ($\Delta T_{flapping}$) for further data reduction. The lift and thrust augmentations refer to the increases of the mean lift and thrust generated by a tested wing in flapping flight compared with those of the same wing in soaring flight (i.e., without flapping motion) with the same forward flight speed and same orientation angle. Subsequently, the coefficients of the lift and thrust augmentations, ΔC_L and ΔC_T, due to flapping motion for a tested wing can be expressed as:

$$\Delta C_L = \frac{\Delta L_{flapping}}{\frac{1}{2}\rho V_\infty^2 S} = \frac{Lift_{flapping} - Lift_{soaring}}{\frac{1}{2}\rho V_\infty^2 S} \tag{2}$$

and

$$\Delta C_T = \frac{\Delta T_{flapping}}{\frac{1}{2}\rho V_\infty^2 S} = \frac{Thrust_{flapping} - Thrust_{soaring}}{\frac{1}{2}\rho V_\infty^2 S}, \tag{3}$$

where S is the platform area of the test wings.

As described by Ho et al. [14], flapping flight can be separated into two regimes: quasi-steady state regime and unsteady state regime. Quasi-steady state flapping flight refers to where a wing flaps at relatively low frequency (or is hardly flapping at all) during the flight; hence the wing tip speed is low compared to the forward flight speed. Larger birds, such as eagles and seagulls, are usually considered to fly in quasi-steady regime since they usually flap their wings quite slowly, tending to have soaring flight as their wings behave more like fixed wings. On the other hand, smaller birds and insects fly in the unsteady state regime with their wings flapping at much higher flapping frequency (e.g., flies and mosquitoes flap their wings at several hundred hertz), and their wingtip speed during the flapping motion is much faster than the forward flight speed. When a flapping flight is in unsteady state regime, the flow motion around the flapping wing is highly unsteady and cannot be approximated by quasi-steady-state assumptions.

Following the work of Ho et al. [14], a non-dimensional parameter, advance ratio, J, which is widely used to characterize aerodynamics of rotorcraft, is used in the present study to characterize the measurement data of the tested wings in flapping flight. Advanced ratio, J, which is defined as the ratio of forward flight speed (i.e., the incoming flow velocity) to the wingtip velocity during flapping flight, can be expressed as:

$$J = \frac{\textit{forward flight speed}}{\textit{wingtip velocity}} = \frac{V_\infty}{2fA}, \tag{4}$$

where f is the wing flapping frequency, and A is the peak-to-peak displacement of the wing tip during the flapping flight. As described in Ho et al. [14], the flow around a flapping wing can be considered quasi-steady when $J > 1.0$, while $J < 1.0$ corresponds to unsteady state regime.

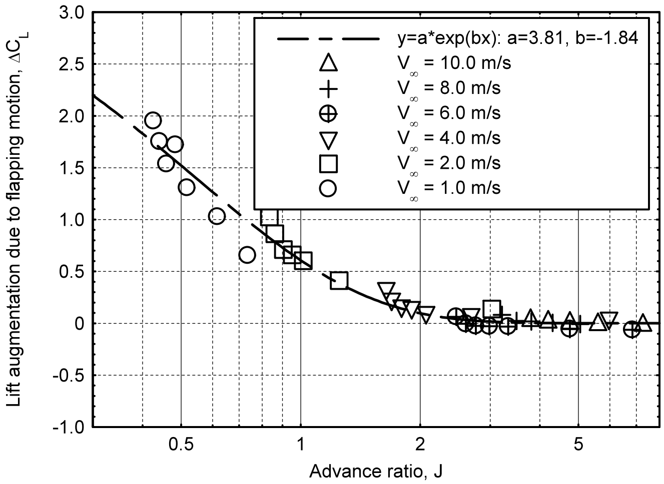

(a). Lift augmentation

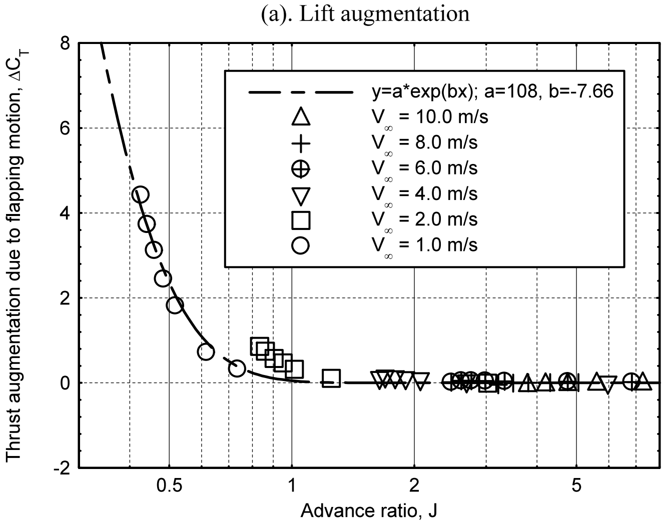

(b). Thrust augmentation

Fig. 9. Lift and thrust augmentations of the rigid wood wing in flapping flight at OA = 10.0 deg.

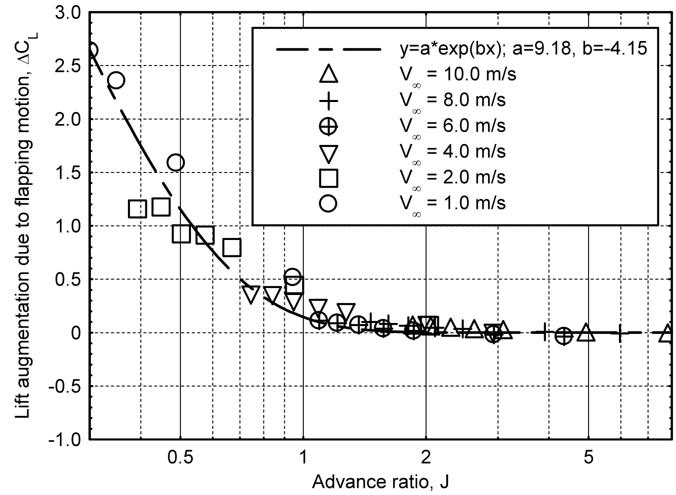

(a). Lift augmentation

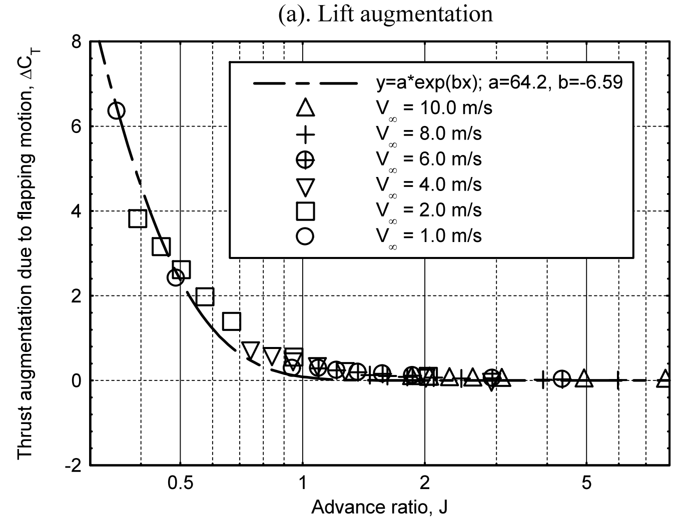

(b). Thrust augmentation

Fig. 10. Lift and thrust augmentation of the flexible nylon wing in flapping flight at OA = 10.0 deg.

It should be noted that Strouhal number, $Str = fA/U_\infty$ or/and reduced frequency, $k = 2\pi fc/U_\infty$, are widely used to characterize the aerodynamic performance of flapping flight [11,19,24,23,36,37,25,5,3,41]. By using non-dimensional flapping amplitude, $h = A/c$, the relationship between the product kh and the Strouhal number (Str) can be written as $kh = 2\pi Str$. Therefore, the advance ratio, J, used in the present study is actually the reciprocal of Strouhal number, i.e., $J = \frac{V_\infty}{2fA} = \frac{\pi}{2kh} = \frac{1}{2Str}$. Since the flapping amplitude A, and chord length C are the same for all the tested wings, the non-dimensional flapping amplitude, $h = A/c$, is a constant in the present study. As a result, the reduced frequency, k, is a linear function of the Strouhal number, Str, which is also the reciprocal function of advance ratio, J.

Based on the flapping flight measurement data shown in Figs. 6–8, the non-dimensional parameters in the terms of coefficients of lift and thrust coefficient augmentations, ΔC_L and ΔC_T, as functions of advance ratio of the flapping flight, J, were calculated. The results were given in Figs. 9–11. It can be seen clearly that, for all three tested wings, the lift and thrust coefficient augmentation data (i.e., ΔC_L and ΔC_T) with different experimental settings (i.e., different flapping frequency and different flight speed, thereby, different Reynolds numbers) were found to align themselves nicely in the plots when the advance ratio, J, was used to reorganize the measurement results. It should be noted that, as shown in Figs. 9–11, the relationships between the lift and thrust coefficient augmentations (i.e., ΔC_L and ΔC_T) and the advance ratio, J, can be represented reasonably well by exponential functions for all the three tested wings. The exponential relationships between the lift and thrust augmentations (i.e., ΔC_L and ΔC_T) with advance ratio of the flapping flight were also confirmed from the measurement data at different orientation angles, though those results were not given here.

One interesting implication deserving further discussion is the effects of the chord Reynolds numbers on the aerodynamic performance of flapping wings/airfoils, since the variation of advance ratio of the flapping flight may also cause the changes of the chord Reynolds numbers. For the cases investigated in the present study, the chord length of the tested wing models are fixed, the comparisons of the measurement results obtained at different flight speed can be used to represent the effects of the chord Reynolds number (i.e. $Re = 10{,}000$ for the case of $V_\infty \approx 1.0$ m/s and $Re \approx 100{,}000$ for the case of $V_\infty = 10.0$ m/s). As shown clearly in Figs. 6–8, the total lift and thrust/drag forces generated by the flapping wings are found to be dependant on flight speed (thereby, chord Reynolds numbers) greatly when the measurement results are presented by using the absolute values of the measured lift and thrust (or drag) forces vs. flapping frequency of the tested wings. However, as shown clearly in Figs. 9–11, when the measurement data were represented by using non-dimensional parameters, i.e., using lift and thrust coefficient augmentations vs. advance ratio, the mea-

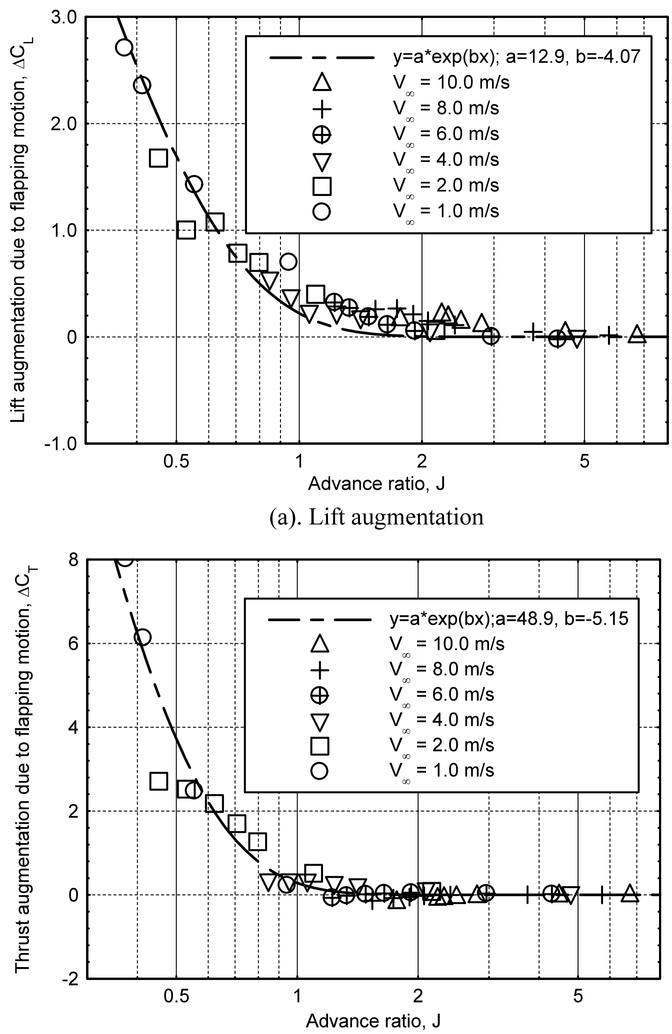

(a). Lift augmentation

(b). Thrust augmentation

Fig. 11. Lift and thrust augmentation for the flexible latex wing in flapping flight at OA = 10.0 deg.

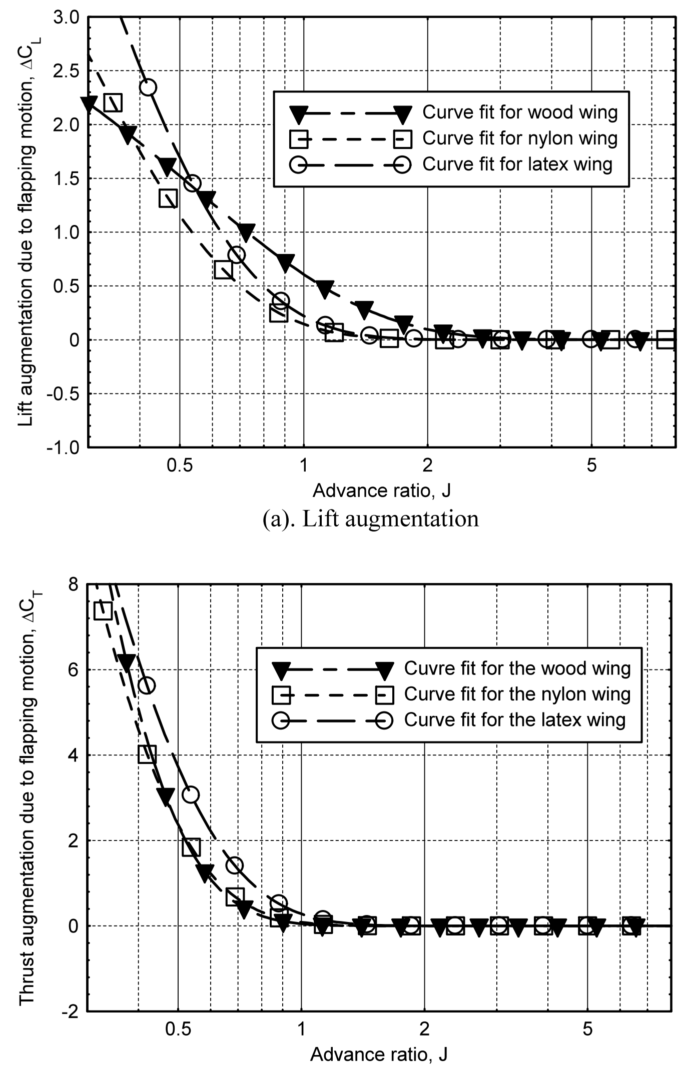

(a). Lift augmentation

(b). Thrust augmentation

Fig. 12. Comparison of the tested wings in flapping flight at OA = 10.0 deg.

surement data obtained at different Reynolds numbers were found to align themselves nicely in the plots, which can be fitted reasonably well by using exponential functions. This indicates that the Reynolds numbers have almost no effects on the aerodynamic performance (i.e., in the terms of lift and thrust/drag coefficients) of the flapping wings when the advance ratio (i.e., Strouhal number and/or reduced frequency) was used to reorganize the measurement results. The finding derived from the present study was found to be consistent with the conclusions reported in previous studies on flapping wings/airfoils [11,19,24,23], i.e., the aerodynamic performance (i.e., the lift and thrust drag coefficients) of a flapping wing/airfoil is almost independent of the Reynolds numbers, as summarized by Ol et al. [24].

As revealed clearly in Figs. 9–11, flapping motion would bring significant aerodynamic benefits (i.e., generate much more lift and thrust) if the flapping flight is in unsteady state regime (i.e. $J < 1.0$). For example, for a flapping flight with the advance ratio $J = 0.50$, the coefficient of the lift augmentation (ΔC_L) due to flapping motion was found to be as high as 1.5, 1.2, and 1.8 for the tested wood wing, nylon wing, and latex wing, respectively. For comparison, as revealed in Fig. 3 and Fig. 4, the lift coefficients for the same tested wings in soaring flight (i.e., without flapping motion) were found to be only about $0.3 \sim 0.6$ at the same orientation angle of OA = 10.0 degrees. It means that, for the same tested wings, the lift production can be increased by a factor of $2.0 \sim 6.0$ by flapping motion when the flapping flight is in unsteady regime with $J = 0.50$. More lift can be produced for the same tested wings as the advance ratio of the flapping flight decreases.

The measurement results also revealed that significant thrust would be generated by flapping motion when the flapping flight is in unsteady state regime. According to the measurement data shown in Figs. 3 and 4, the drag coefficients of the three tested wings in soaring flight would be about $0.05 \sim 0.10$ at OA = 10.0 degrees. The measurement data given in Figs. 9–11 revealed that, with the advance ratio $J = 0.5$, the thrust augmentation (ΔC_T) due to flapping motion would be as high as 2.5, 2.4, and 3.7 for the tested wood wing, flexible nylon wing, and very flexible latex wing respectively. It indicates that the thrust generated by flapping motion would be much larger than the drag acting on the wings. As a result, the resultant aerodynamic forces along the flight direction would be propulsive, which can provide enough power to ensure sufficient maneuverability or/and agility of the flapping flight. This may also be the reason why smaller birds and insects fly in unsteady state regime. For example, the advance ratio of the bumblebee, black fly, and fruit fly in free flight is 0.66, 0.50, and 0.33 respectively [14].

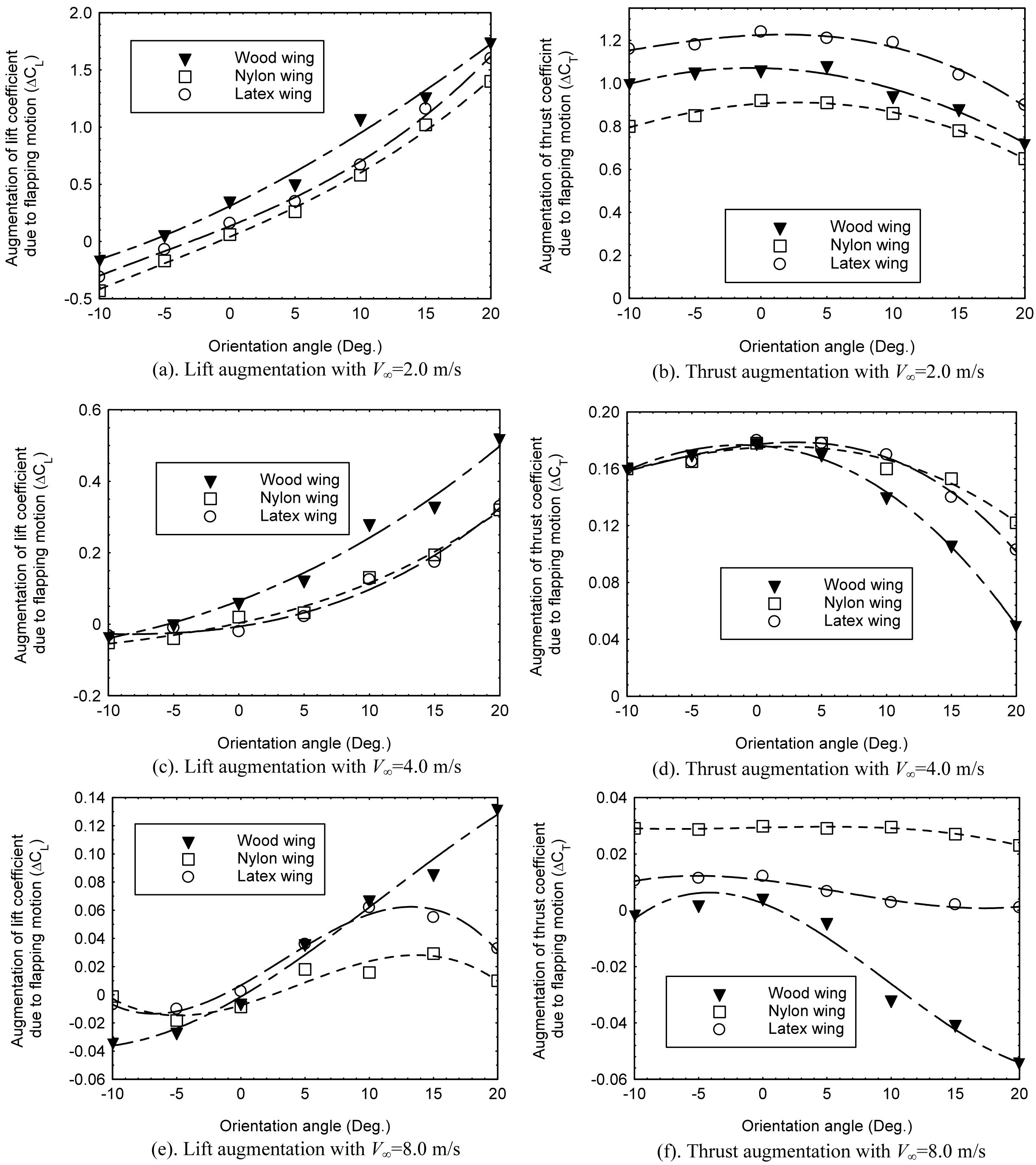

(a). Lift augmentation with V_∞=2.0 m/s

(b). Thrust augmentation with V_∞=2.0 m/s

(c). Lift augmentation with V_∞=4.0 m/s

(d). Thrust augmentation with V_∞=4.0 m/s

(e). Lift augmentation with V_∞=8.0 m/s

(f). Thrust augmentation with V_∞=8.0 m/s

Fig. 13. Effect of the orientation angle (flapping frequency $f = 4.0$ Hz).

On the other hand, since the lift and thrust augmentations due to flapping motion were found to decrease exponentially with the increasing advance ratio of the flapping flight, aerodynamic benefits of flapping flight would be diminished rapidly as the advance ratio of the flapping flight increases. The flapping motion would make very limited or no contributions to either lift augmentation or thrust generation when the flapping flight is in quasi-steady regime with relatively large advance ratio values. For example, for a flapping flight with the advance ratio $J = 2.0$, the aerodynamic benefits due to flapping motion would be almost negligible (i.e., $\Delta C_L < 0.08$, 0.06 and 0.04, and $\Delta C_T < 0.05$, 0.06, and 0.03 for the tested wood wing, nylon wing, and latex wing respectively). It indicates that the aerodynamic forces acting on the tested wings in flapping flight would be almost the same as those in soaring flight (i.e., without any flapping motion).

The exponential curves best-fitted to the measurement data (both lift and thrust) for the three tested wings were plotted on a same graph (Fig. 12) in order to elucidate the effects of skin flexibility of the tested wings on their aerodynamic performances in flapping flight more clearly. It can be seen clearly that, among the three tested wings flapping flight, the rigid wood wing was found to have the best lift generation performance for the flapping flight with relatively large value of advance ratio (i.e., $J > 0.60$). The latex wing, which is most flexible among the three tested wings, would overpass the rigid wing to produce the highest lift for the flapping flight in highly unsteady regime with $J < 0.60$. The nylon wing, which has the best overall aerodynamic performance among the three tested wings for soaring flight, was found to have the worst lift production performance for flapping flight. It can also be seen that, among the three tested wings, the most flexible latex wing was found to have the best thrust augmentation performance for flapping flight. The flexible nylon wing was found to have a comparable thrust generation performance as the rigid wing for flapping flight until highly unsteady flapping flight.

The effects of the orientation angle of the flapping plane on the aerodynamic performances of the tested wings in flapping flight were also investigated in the present study. During the experiments, the flapping frequency of the tested wings was kept as a constant, i.e. $f = 4.0$ Hz, the forward flight speed was varied from $V_\infty = 1.0$ m/s to 10.0 m/s. Fig. 13 shows some typical measurement results with the forward flight speed $V_\infty = 2.0$ m/s, 4.0 m/s, and 8.0 m/s respectively. It should be noted that, for the tested cases with the forward flight speed $V_\infty = 2.0$ m/s, the corresponding advance ratio of the flapping flight is 0.80 (i.e., $J = 0.8$), therefore, the flapping flight is in the unsteady state regime. When the forward flight speed increases to $V_\infty = 4.0$ m/s and 8.0 m/s, the corresponding advance ratios become 1.6 and 3.2, respectively (i.e., $J = 1.6$ and $J = 3.2$), thus, flapping flight is the in quasi-steady regime. As expected, with the same flapping frequency of $f = 4.0$ Hz, the lift and thrust augmentation coefficients of flapping flight in the unsteady state regime (i.e., the case with forward flight speed $V_\infty = 2.0$ m/s) were found to be much higher than those cases in the quasi-steady state regime (i.e., the cases with the forward flight speed $V_\infty = 4.0$ m/s and 8.0 m/s) at all of the tested orientation angles.

The measurement data shown in Fig. 13 revealed that, for all the three tested wings, the lift augmentation coefficients of the three tested wings were found to increase monotonically with the increasing orientation angle when the forward flight speed of the flapping flight was relatively small ($V_\infty < 6.0$ m/s). When the forward flight speed became relatively high ($V_\infty > 6.0$ m/s), the lift augmentation coefficients of the two flexible membrane wings in flapping flight were found to increase at first, reach their peak values at OA $\approx 10.0 \sim 15.0$ deg., then decrease as the orientation angle increases, while the lift augmentation coefficient of the rigid wood wing was still found to increase monotonically with the increasing orientation angle. Among the three tested wings, the rigid wood wing was found to have the best lift production performance for flapping flight at almost all the tested orientation angles. The two tested flexible membrane wings were found to have comparable lift generation performance with the latex wing performing slightly better.

The thrust augmentation coefficient data shown in Fig. 13 revealed clearly that orientation angle would also affect the thrust generation performance of the tested wings in flapping flight greatly. Maximum thrust was found to be generated at OA ≈ 0.0 degree for all three tested wings. The thrust augmentation coefficients due to flapping motion were found to decrease with the increasing orientation angle for all the three test wings. The latex wing, which has the most flexible skin, was found to have the best thrust generation performance among the three tested wings for flapping flight in the unsteady state regime (i.e., the case with $V_\infty = 2.0$ m/s and $J = 0.8$ case). The nylon wing was found to have the best thrust generation performance when the flapping flight was in the quasi-steady regime with a relatively large advance ratio (i.e., $V_\infty = 8.0$ m/s and $J = 3.2$ case). It should also be noted that, for the rigid wing with relatively high forward flight speed (i.e., $V_\infty = 8.0$ m/s and $J = 3.2$), the thrust augmentation data (ΔC_T) was found to become negative at most of the tested orientation angles. It indicates that flapping motion of the rigid wood wing would actually induce additional drag instead of generating thrust. Such measurement results confirmed again that flapping flight would be more aerodynamically efficient when the flapping flight is in the unsteady state regime. The advantages of flapping flight would diminish rapidly with the increasing advance ratio. Flapping motion could even become detrimental for high speed flight applications.

4. Concluding remarks

An experimental study was conducted to assess the aerodynamic benefits of flapping flight compared with fixed-wing soaring flight for the development of flapping-wing Micro-Air-Vehicles (MAVs). The time-averaged aerodynamic performance (i.e. mean lift and thrust/drag) of two flexible membrane wings with different skin flexibilities (i.e., a flexible nylon wing and a more flexible latex wing) were compared with that of a conventional rigid wing in order to assess the effects of skin flexibility of the tested wings on their aerodynamic performances. Advance ratio, which is defined as the ratio of the forward flight speed to the wingtip velocity of the tested wings in flapping flight, was used to do the data reduction to characterize the aerodynamic advantages of flapping flight over soaring flight.

The measurement results revealed clearly that flapping motions could bring significant aerodynamic benefits when the flapping flight is in an unsteady state regime with advance ratio $J < 1.0$. Both lift and thrust augmentations due to flapping motion were found to decrease exponentially as the advance ratio increases, the aerodynamic advantages of flapping flight would diminish rapidly with the increasing advance ratio. Flapping motion could even become detrimental for high speed flight applications.

The orientation angle of the flapping motion with respect to the incoming flow velocity was found to have considerable effects on both the lift and thrust generation of the tested wings in flapping flight. More lift was found to be generated as the orientation angle of the flapping motion increases in general. The tested wings were found to produce maximum thrust when the orientation angle was zero. The thrust generated due to flapping motion would decrease monotonically with the increasing orientation angle.

The skin flexibility of the tested wings was found to affect their aerodynamic performances significantly for both soaring flight and flapping flight. For soaring flight, the flexible membrane wings were found to have better overall aerodynamic performances (i.e., lift-to-drag ratio) in general. The benefits of using flexible membrane wings for soaring flight are much more highlighted for the cases with relatively high forward flight speed and large angles of attack, where the induced deformations for the flexible membrane wings were found to become more obvious. The flexible nylon wing, which has the medium flexibility among the three tested wings, was found to have the best overall aerodynamic performance (i.e., lift-to-drag ratio) for soaring flight.

The rigid wood wing was found to have better lift generation performance compared with the two flexible membrane wings in flapping flight until the flapping flight was in deeply unsteady regime. The latex wing, which is the most flexible wing among the three tested wings, was found to have the best thrust generation performance for flapping flight. The nylon wing, which has the best performance for soaring flight, was found to be the worst for flapping flight applications. Such measurement results imply that it is important to choose proper skin flexibility for the membrane wings in order to achieve improved aerodynamic performances by using flexible membrane airfoils/wings in MAV designs.

It should be noted that, while the measurement results of the present study have revealed that it is possible to augment both lift and thrust significantly by having the flapping flight working in deeply unsteady regime (i.e. $J < 0.50$), the augmentations are usually achieved at the cost of much higher power input. Based on the experimental and numerical investigations of 2-D airfoils in plunge motion, previous studies [3,41] have suggested optimum propulsive efficiencies within an approximate range of $0.20 < Str < 0.4$, which corresponds to the advance ratio of $1.25 < J < 2.5$ for a 2-D flapping airfoil. According to Taylor et al. [36], half of the peak-to-peak flapping amplitude at wingtip can be used to calculate the equivalent Strouhal number (Str) for a 3-D flapping wing, the equivalent advance ratio for efficient propulsion will be about $0.6 < J < 1.25$ for the root-fixed 3-D flapping wings as those used in the present study.

While the present study has revealed many interesting facts related to the aerodynamic performances of flexible membrane wings in soaring and flapping flight, further studies, such as detailed flow field measurements to quantify the vortex structures generated in the wakes of the flapping wings with different structural flexibility, and quantification of the dynamic deformation on flexible membrane wings to exam the flow-structure interactions in flapping cycles, are highly desirable in order to elucidate fundamental physics to further our understanding and to explore/optimize design paradigms for the development of novel flexible membrane-wing-based (either fixed-wing or flapping-wing) MAVs for improved aerodynamic performance.

Acknowledgements

The authors want to thank Mr. Bill Rickard and Mr. Matthew Burkhalter of Iowa State University, Capt. Judson Babcock of AFRL/RWGN, Eglin AFB, and Ms. Pamela Prater of University of West Florida for their help in conducting the experiments. The support of 2008 Air Force Summer Faculty Fellowship Awarded to H. Hu is gratefully acknowledged.

References

[1] M. Abdulrahim, Dynamic characteristics of morphing micro air vehicles, thesis for Master of Science, Department Mechanical and Aerospace Engineering, University of Florida, 2004.

[2] R. Albertani, B. Stanford, J.P. Hubner, P.G. Ifju, Aerodynamic coefficients and deformation measurements on flexible micro air vehicle wings, Experimental Mechanics 47 (2007) 625–635.

[3] J.M. Anderson, K. Streitlien, D.S. Barrett, M.S. Triantafyllou, Oscillating foils of high propulsive efficiency, Journal of Fluid Mechanics 360 (1998) 41–72.

[4] S.A. Ansari, R. Zbikowski, K. Knowles, Aerodynamic modeling of insect-like flapping flight for micro air vehicles, Progress in Aerospace Sciences 42 (2006) 129–172.

[5] D.G. Bohl, M.M. Koochesfahani, MTV measurements of the vortical field in the wake of an airfoil oscillating at high reduced frequency, Journal of Fluid Mechanics 620 (2009) 63–88.

[6] F. Bohorquez, P. Samuel, J. Sirohi, D. Pines, L. Rudd, R. Perel, Design analysis and Hover performance of a rotating wing micro air vehicle, Journal of the American Helicopter Society 48 (2) (2003) 80–90.

[7] K.P. Dial, An inside look at how birds fly: experimental studies of the internal and external processes controlling flight, 1994 Report the Aerospace Profession, 38th Symposium Proceedings, The Beverly Hilton, Beverly Hills, CA, 1994.

[8] M.H. Dickinson, K.G. Götz, Unsteady aerodynamic performance of model wings at low Reynolds numbers, Journal of Experimental Biology 174 (1993) 45–64.

[9] M.H. Dickinson, F.-O. Lehmann, S. Sane, Wing rotation and the aerodynamic basis of insect flight, Science 284 (1999) 1954–1960.

[10] C.P. Ellington, C. van den Berg, A.P. Willmott, A.L.R. Thomas, Leading-edge vortices in insect flight, Nature 384 (1996) 626–630.

[11] D. Garmann, M. Visbal, High fidelity simulations of transitional flow over pitching airfoils, AIAA 2009-3693, 2009.

[12] S. Heathcote, D. Martin, I. Gursul, Flexible flapping airfoil propulsion at zero freestream velocity, AIAA Journal 42 (11) (2004) 2196–2204.

[13] S. Heathcote, Z. Wang, I. Gursul, Effect of spanwise flexibility on flapping wing propulsion, Journal of Fluids and Structures 24 (2) (2008) 183–199.

[14] S. Ho, H. Nassef, N. Pornsinsirirak, Y. Tai, C.M. Ho, Unsteady aerodynamics and flow control for flapping wing flyers, Progress in Aerospace Sciences 39 (2003) 635–668.

[15] Y.S. Hong, A. Altman, Lift from spanwise flow in simple flapping wings, Journal of Aircraft 45 (4) (2008) 1206–1216.

[16] H. Hu, M. Tamai, J.T. Murphy, Flexible membrane airfoils at low Reynolds numbers, Journal of Aircraft 47 (5) (2008) 1767–1778.

[17] T. Hubel, N. Hristov, S. Swartz, K. Breuer, Time-resolved wake structure and kinematics of bat flight, Experiments in Fluids 46 (5) (2009) 933–943.

[18] K.M. Isaac, J. Rolwes, A. Colozza, Aerodynamics of a flapping and pitching wing using simulations and experiments, AIAA Journal 46 (6) (2008) 1505–1515.

[19] Y. Lian, Parametric study of a pitching flat plate at low Reynolds numbers, AIAA 2009-3688, 2009.

[20] M.J. Lighthill, On the Weis-Fogh mechanism of lift generation, Journal of Fluid Mechanics 60 (1973) 1–17.

[21] T. Maxworthy, Experiments on the Weis-Fogh mechanism of lift generation by insects in hovering flight. Part 1. Dynamics of the fling, Journal of Fluid Mechanics 93 (1979) 47–63.

[22] T.J. Mueller (Ed.), Fixed and Flapping Wing Aerodynamics for Micro Air Vehicle Applications, Progress in Astronautics and Aeronautics, AIAA, Reston, VA, 2001.

[23] M. Ol, The high-frequency, high-amplitude pitch problem: Airfoils, plates and wings, AIAA 2009-3686, 2009.

[24] M. Ol, A. Altman, J. Eldredge, D. Garmann, Y. Lian, Summary of progress on pitching plates: Canonical problems in low-re unsteady aerodynamics, AIAA-2010-1085, 2010.

[25] M.E. Platzer, K.D. Jones, J. Yong, J.C.S. Lai, Flapping wing aerodynamics: Progress and challenges, AIAA Journal 46 (9) (2008) 2136–2149.

[26] M. Ramasamy, J.G. Leishman, T.E. Lee, Flow field of a rotating wing MAV, in: Proceedings of 62nd Annual National Forum of the American Helicopter Society, 2006.

[27] W. Shyy, M. Berg, D. Ljunqvist, Flapping and flexible wings for biological and micro air vehicles, Progress in Aerospace Sciences 35 (1999) 455–506.

[28] W. Shyy, P. Ifju, D. Viieru, Membrane wing-based micro air vehicles, Applied Mechanics Reviews 58 (2005) 283–301.

[29] W. Shyy, D.A. Jenkins, R.W. Smith, Study of adaptive shape airfoils at low Reynolds number in oscillatory flows, AIAA Journal 35 (1997) 1545–1548.

[30] W. Shyy, Y. Lian, J. Tang, D. Viieru, H. Liu, Aerodynamics of Low Reynolds Number Flyers, Cambridge University Press, 2008.

[31] R.W. Smith, W. Shyy, Computation of unsteady laminar flow over a flexible two-dimensional membrane wing, Physics of Fluids 7 (1995) 2175–2184.

[32] A. Song, X. Tian, E. Israeli, R. Galvao, K. Bishop, S. Swartz, K. Breuer, Aeromechanics of membrane wings, with implications for animal flight, AIAA Journal 46 (8) (2008) 2096–2196.

[33] B. Stanford, P. Ifju, R. Albertani, W. Shyy, Fixed membrane wings for micro air vehicles: Experimental characterization, numerical modeling, and tailoring, Progress in Aerospace Sciences 44 (2008) 258–294.

[34] M. Sun, J. Tang, Unsteady aerodynamic force generation by a model fruit fly wing in flapping motion, Journal of Experimental Biology 205 (2002) 55–70.

[35] M. Sun, J. Tang, Lift and power requirements of hovering flight in Drosophila virilis, Journal of Experimental Biology 205 (2002) 2413–2427.

[36] G.K. Taylor, R.L. Nudds, A.L.R. Thomas, Flying and swimming animals cruise at a Strouhal number tuned for high power efficiency, Nature 425 (2003) 707–711.

[37] G.S. Triantafyllou, M.S. Triantafyllou, M.A. Grosenbaugh, Optimal thrust development in oscillating foils with application to fish propulsion, Journal of Fluids Structure 7 (1993) 205–224.

[38] D. Viieru, J. Tang, Y. Lian, H. Liu, W. Shyy, Flapping and flexible wing aerodynamics of low Reynolds number flight vehicles, AIAA paper 2006-0503.

[39] Z.J. Wang, J.M. Birch, M.H. Dickinson, Unsteady forces and flows in low Reynolds number hovering flight: Two-dimensional computations vs robotic wing experiments, Journal of Experimental Biology 207 (2004) 449–460.

[40] T. Weis-Fogh, Quick estimate of flight fitness in hovering animals, including novel mechanisms for lift production, Journal of Experimental Biology 59 (1973) 169–230.

[41] J. Young, J.C.S. Lai, Mechanisms influencing the efficiency of oscillating airfoil propulsion, AIAA Journal 45 (7) (2007) 1695–1702.